

Pseudo-3D Trajectories: An Effective Approach for Motion Representation in Depth Data

Author1's name

Adress 1

Author2's name

Adress 2

Author3's name

Adress 3

Abstract

Leveraging the motion information of trajectories shows the effectiveness to the human action recognition in intensity videos. However, the influence of this approach for representing motions in depth video is not still answered. In this paper, we will deal with this issue by conducting experiments based on intensity trajectory features to describe motion information in depth video. In addition, in order to ensure including depth information, we propose a method based on compensating motion information from different representations of depth video. Evaluated on benchmark datasets, our method significantly outperforms the state-of-the-art depth-based methods.

Keywords: Trajectory, action recognition, depth data, feature representation

1. Introduction

Action recognition in videos has been one of the very active research fields in computer vision [1, 2] due to its wide applications in areas like surveillance, video retrieval, human-computer interaction and smart environments. In the recent
5 decades, studies of human action recognition mainly work on video sequences captured by traditional RGB cameras. Because of individual differences, the diversity and complexity of actions, and complex backgrounds, action recognition is still a challenging problem. In domain of 2D videos, two approaches are used popularly, including: spatio-temporal interest points (STIP)-based ap-
10 proach and trajectory-based approach. The first approach, as described in works [13–18], generates a compact video representation and accepts background clutter, occlusions and scale changes. However, in case of recognizing complicated motions, the approach deals with several challenges, due to the lack of relationship of interest points. In recent studies [19–21], an other approach based on
15 trajectories captures moving patterns in video, thereby it provides additional information to recognize motions more exactly. H.Wang et al. [24] has demonstrated that dense trajectory-based approach is the state-of-the-art approach for action recognition.

With the development of new RGB-D cameras, e.g. Kinect camera, capturing
20 color images as well as depth maps has become feasible in real time. The depth maps can provide additional cues, such as body shape and motion information to discriminate actions. Due to these advantages, recent research trend concentrates on exploiting depth maps for action recognition [3–12]. In our best knowledge, none success with combining dense trajectories, the state-of-the-art
25 approach on 2D video, and depth video. In this paper, we investigate to exploit the dense trajectory-based approach on depth video.

In order to exploit the 2D approach on depth video, we must transform depth video to corresponding 2D video. This issue can be easily performed by considering depth value as intensity value. However, this way can cause

30 confused cases of action classes. For example, forward punch and hammer may be confused actions, if we view them from front, since they contain similar movements respectively: lift arm up and stretch out. Therefore the additional information is needed to distinguish such actions.

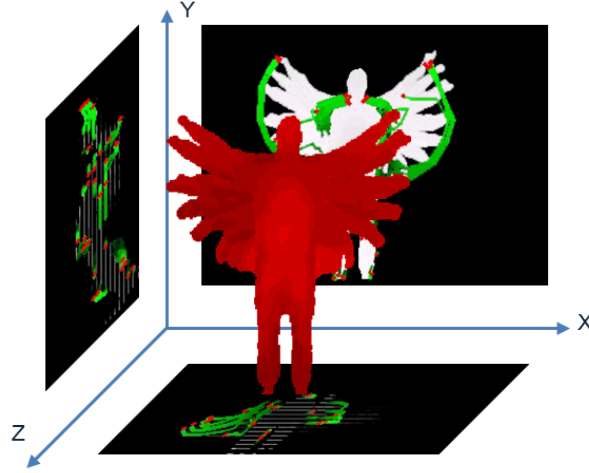


Figure 1: Illustration of our trajectory-based approach. The original sequence of depth maps is projected onto three orthogonal planes to form intensity videos. After that, the dense trajectory motion features are calculated for each representation.

The basis idea to deal with such cases is to watch actions from various views.
 35 Information achieved from the views can provide clearer cues to discriminate such actions. To collect such information from depth video, a simple way is to project depth maps onto view planes, see figure 1. The projections are easily obtained by the mentioned advantages of depth data. Data projected on the planes is then gathered to generate corresponding 2D videos. Dense trajectory-
 40 based motion features are then calculated on 2D videos to generate a final feature representation for depth video.

To evaluate the effectiveness of our method, we conduct experiments on MSR Action 3D dataset and MSR Daily Activity 3D dataset. Experimental

results show that our proposed method beats the state-of-the-art methods in
 45 constrain of only using depth data. The results also present our contributions:
 (1) we propose an effective method to exploit trajectories in depth video, (2)
 we perform comprehensive experiments on the challenging benchmark dataset
 and indicate that our proposed method is the best when compared with the
 state-of-the-art depth-based methods.

50 After a brief review of the related work in Section 2, the proposed method is
 described in Section 3. Sections 4 and 5 present the experimental settings and
 results. In section 6 we provide some concerned discussions. The summaries of
 our work are given in Section 7.

2. Related Works

55 In terms of human action recognition in depth video, most recent methods
 exploit depth information into two major directions. The first one is adapting
 intensity techniques-based methods for depth data. The second one is to use
 depth value as its mean.

For the first direction, Yang.X et al. [6] propose the Depth Motion Maps
 60 (DMM) to accumulate global activities in depth video sequences. The DMM
 are generated by stacking motion energy of depth maps projected onto three
 orthogonal Cartesian planes. And the Histogram of Oriented Gradients (HOG)
 [22] are computed from the DMM to represent an action video. Another ap-
 proach proposed by Xia.L and Aggarwal.J.K [9] presents a filtering method to
 65 extract spatio-temporal interest points from depth videos (DSTIPs). In this ap-
 proach, they extend a work of Dollar et al. [14] to adapt for depth data. Firstly,
 2D and 1D filters (e.g. Gaussian and Gabor filters) are applied respectively on
 to the spatial dimensions and temporal dimension in depth video. A correction
 function then is used to suppress points as depth noises. Finally, points with
 70 the largest responses by this filtering method will be selected as the DSTIPs for

each video. Besides, a depth cuboid similarity feature (DCSF) is proposed to describe a 3D cuboid around the DSTIPs with supporting size to be adaptable to the depth.

For the second direction, [3] used a bag of 3D points to characterize a set
75 of salient postures. The 3D points are extracted on the contours of the planar projections of the 3D depth map. And then, about 1% 3D points are sampled to calculate feature. Unlike [3], [4, 11, 12] use occupancy patterns to represent features in action videos.

Vieira et al. [11] proposed a new feature descriptor, called Space-Time Oc-
80 cupancy Patterns (STOP). This descriptor is formed by sparse cells divided by the sequence of depth maps in a 4D space-time grid. The values of the sparse cells are determined by points inside to be on the silhouettes or moving parts of the body. Wang et al. [12] presented semi-local features called Random Occupancy Pattern (ROP) features from randomly sampled 4D sub-volumes
85 with different sizes and different locations. The random sampling is performed under a weighted scheme to effectively explore the large dense sampling space. Besides, authors also apply a sparse coding approach to robustly encode these features. The work by Wang et al. [4] designed a feature to describe the local “depth appearance” for each joint, named Local Occupancy Patterns (LOP). The
90 LOP features are computed based on 3D point cloud around a particular joint. Moreover, they concatenate the LOP features with skeleton information-based features and apply Short Fourier Transform to obtain the Fourier Temporal Pyramid features at each joint. The Fourier features are utilized in a novel actionlet ensemble model to represent each action video.

95 Recently, Oreifej and Liu [10] presented a new descriptor for depth maps, named Histogram of Oriented 4D Surface Normals (HON4D). To construct the HON4D, firstly, the 4D normal vectors are computed from the depth sequence. At the next step, the 4D normal vectors is distributed into spatio-temporal cells. To quantize the 4D normal vectors, the 4D space is quantized by using vertices of

100 a regular polychoron. The quantization, then, is refined by additional projectors to make the 4D normal vectors in each cell denser and more discriminative. Afterwards, the HON4D features in cells are concatenated to represent a depth action video.

Inspired by results of Shotton et al. [23] and Xia.L et al. [7], the work
105 by Yang et al. [5] developed the EigenJoints features based on skeleton information from RGBD sequences. The features contain three feature channels: posture, motion and offset. The posture and motion features represent spatial and temporal information, respectively. The offset features encode the difference between a pose with the initial pose in assumption that the initial pose
110 is neutral. The three channels, then, are normalized and reduced by applying PCA method to obtain the EigenJoints descriptor.

Different from the previous approaches, we use a trajectory-based approach for action recognition. We do not care to segment human body like [3, 6]. Besides, skeleton extraction used in [4, 5] is not also required in our work. We
115 only investigate the benefit of generating intensity representations from depth data, as mentioned in [3, 6]. Moreover, we leverage the effectiveness of trajectory feature to represent an action video. In our best knowledge, no method has previously proposed adapting trajectory-based approach for human action recognition in depth video. We conduct evaluations on recognition accuracy
120 using dense trajectories motion feature proposed by Wang et al. [24].

3. Proposed Method

This paper presents a effective depth video representation by adapting intensity trajectories-based motion features. First, we provide a brief review of the dense trajectory-based feature proposed by Wang.H et al. [24]. Related parts,
125 such as: dense sampling, tracking and feature descriptors are also referred to. Our trajectories-based approach for depth data is mentioned at the end of this

section.

3.1. Dense trajectories

Trajectories provide a compact representation of motion information in video.
 130 Trajectories from intensity videos can be used for MED, video mining, action
 classification and so on. Trajectory extraction much depends on both processes:
 sampling and tracking. Some concerned methods, such as [19, 20] used KLT
 tracker [25], or [21] matched SIFT descriptors between consecutive frames to
 obtain feature trajectories. Recently, the dense trajectories feature proposed
 135 by [24] has achieved state-of-the-art performances on MED systems, such as,
 segment-based system [26] on TRECVID MED 2010, 2011, or AXES [27], and
 BBNVISER [28] on TRECVID MED 2012.

In order to obtain trajectories, there are two important steps: sampling and
 tracking. [24] propose sampling on a dense grid with a step size of 5 pixels.
 140 The sampling is performed at multiple scales with a factor of $1/\sqrt{2}$. Then,
 tracking is the next step to form trajectories. At each scale, in frame t , each
 point $P_t = (x_t, y_t)$ is tracked to point $P_{t+1} = (x_{t+1}, y_{t+1})$ in next frame $t+1$ by:

$$P_{t+1} = (x_{t+1}, y_{t+1}) = (x_t, y_t) + (M * \omega)|_{(\bar{x}_t, \bar{y}_t)}, \quad (1)$$

where $\omega = (u_t, v_t)$ denotes the dense optical flow field, M is the kernel of median
 145 filtering, and (\bar{x}_t, \bar{y}_t) is the rounded position of P_t . The algorithm of [29] is
 adopted to compute the dense optical flow. And to avoid a drifting problem, a
 suitable value of trajectory length is set to 15 frames. Besides, trajectories with
 sudden changes are removed.

After extracting trajectories, two kinds of descriptors: a trajectory shape
 150 descriptor and a trajectory-aligned descriptor can be adopted. In our experi-
 ments, we only use trajectory-aligned descriptors including the HOG [22], the
 Histogram of Optical Flow (HOF) [15], and the Motion Boundary Histogram

(MBH) [30]. HOG captures local appearance information, while HOF and MBH encode local motion pattern. The descriptors are computed within a space-time
155 volume ($N \times N$ spatial pixels and L temporal frames) around the trajectory. This volume is divided into a 3D grid (spatially $n_\sigma \times n_\sigma$ grid and temporally n_τ segments). The default settings of these parameters are $N = 32$ pixels, $L = 15$ frames, $n_\sigma = 2$, and $n_\tau = 3$.

According to the authors [15, 24, 31, 32], all the three descriptors have shown
160 the effectiveness for action recognition. The experimental settings for these descriptors are based on an empirical study showed in [24]. We also conduct our experiment on all the three descriptors when compared to the depth-based state-of-the-art methods.

3.2. Pseudo-3D trajectory-based Approach for Motion Feature in Depth Data

Our proposed trajectory-based approach for human action recognition in
165 depth data is as follow. At first, intensity representations are formed from the sequence of depth maps, as illustrated in figure 1. At this step, to obtain an intensity representation from an view direction α , corresponding to a view plane $\mathcal{P}(\alpha) : ax + by + cz + d = 0$, in each depth map t , each point $P_t(x_t, y_t, z_t)$ is
170 projected to $P_{\mathcal{P}}(x_{\mathcal{P}}, y_{\mathcal{P}}, z_{\mathcal{P}})$ on the view plane $\mathcal{P}(\alpha)$ by:

$$P_t(x_t, y_t, z_t) \xrightarrow{\mathcal{P}(\alpha)} P_{\mathcal{P}}(x_{\mathcal{P}}, y_{\mathcal{P}}, z_{\mathcal{P}}) \quad (2)$$

where,

$$x_{\mathcal{P}} = x_t - \frac{ax_t + by_t + cz_t + d}{a^2 + b^2 + c^2}a \quad (3)$$

$$y_{\mathcal{P}} = y_t - \frac{ax_t + by_t + cz_t + d}{a^2 + b^2 + c^2}b \quad (4)$$

$$z_{\mathcal{P}} = z_t - \frac{ax_t + by_t + cz_t + d}{a^2 + b^2 + c^2}c \quad (5)$$

And the intensity value v at the projected point $P_{\mathcal{P}}$ is computed by:

$$v(P_{\mathcal{P}}) = \frac{ax_t + by_t + cz_t + d}{\sqrt{a^2 + b^2 + c^2}} \quad (6)$$

175 So, given a set of 3D points $\mathcal{S}(t) = \{(x_t, y_t, z_t) | (x_t, y_t, z_t) \in t\}$, we have a projection $\mathcal{S}_{\alpha}(t) = \{(x_{\mathcal{P}}, y_{\mathcal{P}}, z_{\mathcal{P}}) | (x_{\mathcal{P}}, y_{\mathcal{P}}, z_{\mathcal{P}}) \in \mathcal{P}(\alpha)\}$. Therefore, a set of the projections obtained from a given sequence of M depth maps under a view direction α is a expected intensity representation $\mathcal{R}(\alpha) = \{\mathcal{S}_{\alpha}(t) | t = \overline{1..M}\}$.

180 In particular, we choose three representations to represents for three view directions: front, side, and top in 3D space, corresponding to three view planes, respectively: Oxy , Oyz and Ozx . With these view directions, the corresponding projections are respectively:

$$\mathcal{S}_{\text{front}}(t) = \{(x_t, y_t, 0) | (x_t, y_t, 0) \in \mathcal{P} : z = 0\} \quad (7)$$

$$\mathcal{S}_{\text{side}}(t) = \{(0, y_t, z_t) | (0, y_t, z_t) \in \mathcal{P} : x = 0\} \quad (8)$$

$$\mathcal{S}_{\text{top}}(t) = \{(x_t, 0, z_t) | (x_t, 0, z_t) \in \mathcal{P} : y = 0\} \quad (9)$$

185 And the corresponding intensity values in the three projections are, respectively:

$$v(P_{\text{front}}) = z_t \quad (10)$$

$$v(P_{\text{side}}) = x_t \quad (11)$$

$$v(P_{\text{top}}) = y_t \quad (12)$$

190 Forming the representations is necessary due to dimensional gap when we adapt 2D techniques for 3D data. Afterwards, the dense trajectories [24] are extracted from the intensity representations. With this approach, we do not care the challenges from human body segmentation as well as skeleton extraction. Trajectory-aligned descriptors are computed then. At the next step, with

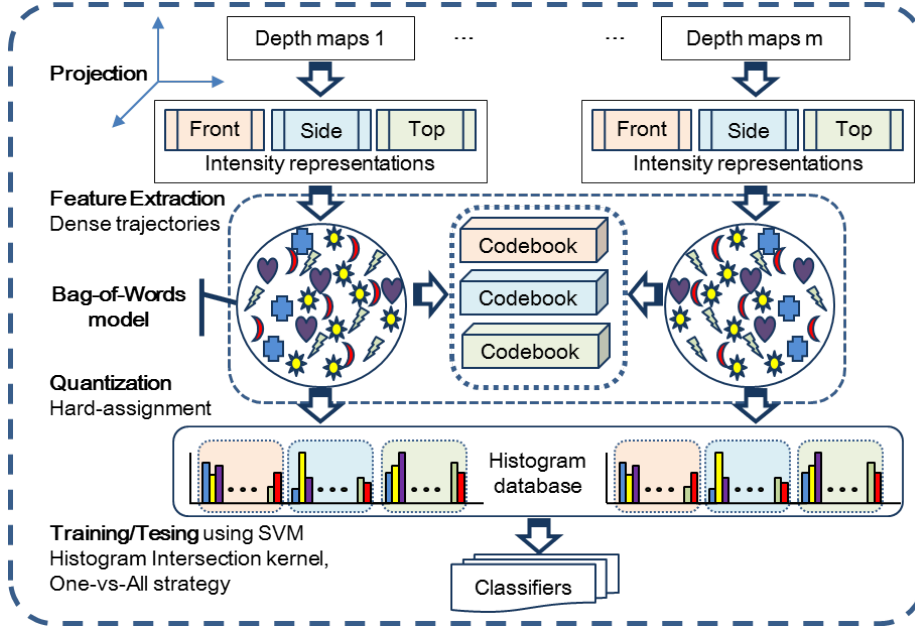


Figure 2: Our Framework Overview

each intensity representation $\mathcal{R}(\alpha_i)$, $i = \overline{1..N}$, corresponding feature representation $F(\alpha_i) = (b_{\alpha_i}^1, b_{\alpha_i}^2, \dots, b_{\alpha_i}^K)$ is quantized from a set of raw trajectory features using a bag-of-words (BoW) model with K visual words. For quantization, the hard-assignment technique is used to compute histograms of the visual words on the corresponding intensity representations. An *early fusion* scheme which integrates unimodal features before learning, then, is used to generate feature representation $\mathcal{F} = (F(\alpha_1), \dots, F(\alpha_N))$ for action in the sequence of depth maps. After the final feature representations are generated, we adopt the popular Support Vector Machine (SVM) for classification. In practice, we use the precomputed-kernel technique with the histogram intersection kernel for the classification step. Besides, we perform the one-vs-all strategy for multi-class classification.

Our proposed trajectory-based approach is compared with the state-of-the-art methods in human action recognition using depth data. Actually, our ap-

proach does not care skeleton extraction, which is used as an important factor in some works, such as [4, 5]. In fact, extracting skeleton exactly is still an completely unsolved problem, due to the challenges, such as cluttered background, hardware quality, camera motion, so on.

4. Experimental Settings

4.1. Dataset

We test our method on MSR Action 3D dataset. This dataset contains 20 actions, as showed in Table 1. Actions are performed by ten subjects for two or three times in the context of game console interaction. In total, there are 567 sequences of depth maps. The depth maps are shot at frame rate of 15 fps. The size of the depth map is 640×480 , we resize into 320×240 to ensure processing efficiency.

ID	Action Name	ID	Action Name
1	high arm wave	11	two hand wave
2	horizontal arm wave	12	side-boxing
3	hammer	13	bend
4	hand catch	14	forward kick
5	forward punch	15	side kick
6	high throw	16	jogging
7	draw x	17	tennis swing
8	draw tick	18	tennis serve
9	draw circle	19	golf swing
10	hand clap	20	pick up & throw

Table 1: 20 actions in MSR Action 3D dataset

In order to conduct a fair comparison, we use the same experimental settings

Action Subset 1 (AS1)	Action Subset 2 (AS2)	Action Subset 3 (AS3)
horizontal arm wave	high arm wave	high throw
hammer	hand catch	forward kick
forward punch	draw x	side kick
high throw	draw tick	jogging
hand clap	draw circle	tennis swing
bend	two hand wave	tennis serve
tennis serve	side-boxing	golf swing
pick up & throw	forward kick	pick up & throw

Table 2: The three action subsets used in the experiments

as [3–6, 9, 10]. In the settings, the dataset is divided into three action subsets. Each subset has 8 actions (Table 2). The two subsets AS1 and AS2 present that grouped actions have similar movements. The subset AS3 groups complex actions together. For instance, action *hammer* seems to be confused with action
225 *forward punch* in AS1 or similar movements between action *hand catch* and action *side boxing* in AS2. As for each subset, we select half of the subjects as training and the rest as testing (i.e. cross subject test).

4.2. Evaluation Framework

Figure 2 shows our evaluation framework for the trajectory-based features.
230 We perform experiments using the proposed approach and compare with the state-of-the-art methods on depth data. We use the application available on-line¹ to extract dense trajectories and aligned-descriptors. Experimental results reported in section 5 attach to the MBH descriptor. The HOG, HOF descriptors will be mentioned in the section 6. To quantize a large number of features

¹http://lear.inrialpes.fr/~wang/dense_trajectories

235 obtained by densely sampling, the BoW model is applied. At first, in each intensity representation, we randomly get about 80,000 extracted trajectories for clustering with K-mean algorithm. Then, a codebook of 2000 visual codewords is formed for each.

In order to classify actions, in our implementation, we use the libSVM library
240 published online by author². We adopt the format requirements of the library to synchronize the annotation and the data. For testing, predicted value of each action is defined as the maximum score obtained from all the classifiers. This score shows that a human action is confused with another or not.

5. Experimental Results

245 This section presents the experimental results for applying our proposed approach on MSR Action 3D dataset. All experimental results are reported under the settings mentioned in section 4.1. Besides, in comparison with the state-of-the-art methods, our reported result is calculated on front representation only. In addition, an evaluation related to selecting compensation information from
250 other representations will be also mentioned. All the results are compared in terms of recognition accuracy. The best performance is highlighted in bold.

5.1. Recognize Actions from An Intensity Representation

Table 3 shows evaluation results of our trajectory-based approach and the state-of-the-art methods in terms of average accuracy on three action subsets
255 of MSR Action 3D dataset (Table 2). The compared methods are based on various feature representations, such as silhouette features [3, 6], skeletal joint features like [4, 5], local occupancy patterns [11, 12], normal orientation features [10] and cuboid similarity features [9]. Interestingly, under the same setting (i.e

²<http://www.csie.ntu.edu.tw/~cjlin/libsvm/>

Method	Accuracy (%)
Bag of 3D Points [3]	74.70
STOP [11]	84.80
EigenJoints [5]	82.33
Random Occupancy Patterns [12]	86.50
Local Occupancy Patterns [4]	88.20
Depth Motion Maps-based HOG [6]	91.63
Histogram of Oriented 4D Normals [10]	88.89
Depth Cuboid Similarity Feature [9]	89.30
Ours	94.53

Table 3: Comparison of accuracy on MSR Action 3D dataset. Notice that experimental results reported in this table is based on front representation only. Besides, we also use MBH descriptor only to calculate trajectory features.

cross subject test), the result table indicates that our approach beats all of
260 them. Besides, the results also show that there is significant difference of the
performance between our method and the rest.

Consider the accuracy results on action subsets reported in Table 4, we
found that two subsets AS1, AS2 contain many confused actions. Considering
confusion matrices as showed in Table 5, some action-pairs are confused, such
265 as: *hammer* (a03) and *forward punch* (a05) in AS1, or *side-boxing* (a12) and
hand catch (a04) in AS2. When analyzing the confused actions, we found that
the main cause is due to similar motions of actions in the same view direction
(i.e front representation). Besides, since depth data is textureless, it makes
recognizing more difficult. That is reason why we need compensate information
270 from other intensity representations.

Action Subsets		
AS1	AS2	AS3
92.45	92.04	99.11

Table 4: Accuracy of our method on three action subsets.

5.2. *Compensate Motion Information from Other Representations*

In this part, we conduct experiments based on compensating information from other representations (i.e side and top) for the front representation. We report the experimental results on three action subsets and the average of the three subsets. Figure 3 shows a better view in comparing the fusion of front, side and top representations with the separate representations. Expectedly, the average recognition accuracy of the fusion, which is 96.67% accuracy, is better than the average recognition accuracy of the representations on the average of the three action subsets. Obviously, our proposed approach outperforms the mentioned state-of-the-art methods.

Besides, based on experimental results in figure 3, compensating information indicates two interesting points. The first one confirms that recognition result from front representation is better than the others (i.e. side and top). The second one shows that compensated information from other representations for front representation supports final predictions effectively. Thus, our proposed approach can be applied for any intensity-based techniques, in general.

	a02	a03	a05	a06	a10	a13	a18	a20
a02	0.83	0	0.17	0	0	0	0	0
a03	0	0.92	0.08	0	0	0	0	0
a05	0	0.36	0.64	0	0	0	0	0
a06	0	0	0	1.0	0	0	0	0
a10	0	0	0	0	1.0	0	0	0
a13	0	0	0	0	0	1.0	0	0
a18	0	0	0	0	0	0	1.0	0
a20	0	0	0	0	0	0.07	0	0.93

(a) Action Subset 1

	a01	a04	a07	a08	a09	a11	a12	a14
a01	1.0	0	0	0	0	0	0	0
a04	0.08	0.84	0.08	0	0	0	0	0
a07	0	0	0.79	0.07	0.07	0	0.07	0
a08	0	0	0	1.0	0	0	0	0
a09	0	0	0	0.13	0.87	0	0	0
a11	0	0	0	0	0	1.0	0	0
a12	0	0.13	0	0	0	0	0.87	0
a14	0	0	0	0	0	0	0	1.0

(b) Action Subset 2

	a06	a14	a15	a16	a17	a18	a19	a20
a06	1.0	0	0	0	0	0	0	0
a14	0	1.0	0	0	0	0	0	0
a15	0	0	1.0	0	0	0	0	0
a16	0	0	0	1.0	0	0	0	0
a17	0	0	0	0	1.0	0	0	0
a18	0	0	0	0	0	0.93	0.07	0
a19	0	0	0	0	0	0	1.0	0
a20	0	0	0	0	0	0	0	1.0

(c) Action Subset 3

Table 5: Confusion matrices on three action subsets. Notice that action names are identified by indices of actions in table 1

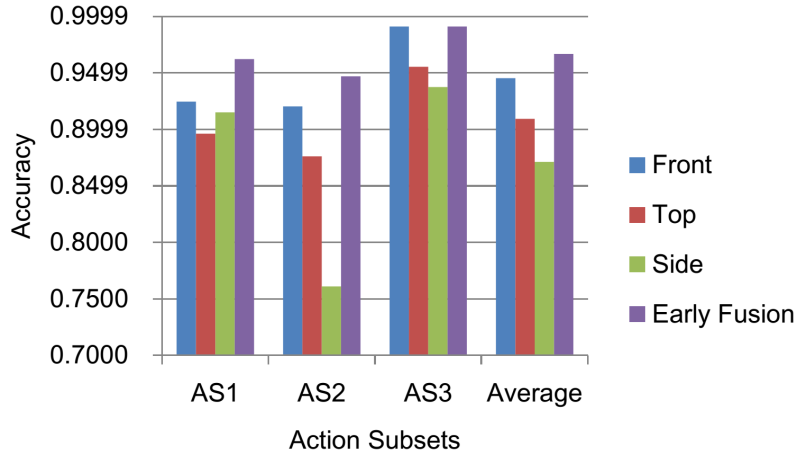


Figure 3: Comparison of recognition accuracy by using the early fusion scheme on intensity representations.

6. Discussions

6.1. The Impact of Our Method on Descriptors

For intensity data, according to [24] MBH is the best feature descriptor for
 290 dense trajectories. Therefore, in previous experiments, we only use MBH de-
 scriptor to represent motion information. Due to the difference between depth
 data and intensity data, how our approach has influenced other trajectory-
 aligned descriptors (i.e. HOG, HOF). In this section, we conduct similar exper-
 iments on these descriptors to answer this issue.

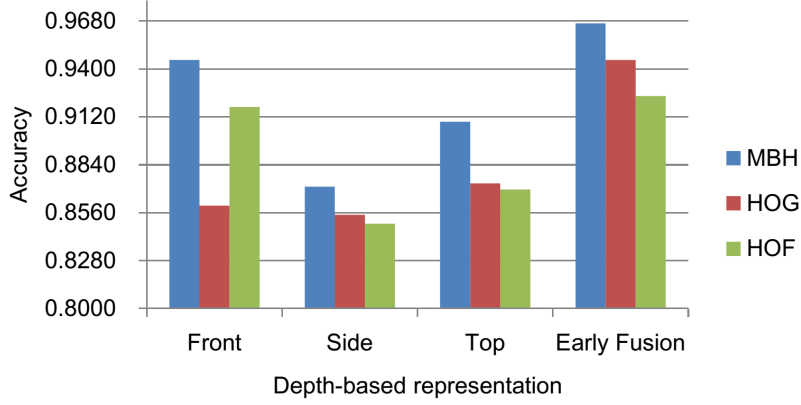


Figure 4: Comparison of recognition accuracy on trajectory-aligned descriptors.

295 In this part, we report the average recognition accuracies on the three descriptors and on the separate representations (i.e. front, side and top) as well as the fusion of the three representations. Figure 4 shows interesting results. Although, recognition results on descriptors HOG, HOF are not good for each intensity representation, the final results after fusing have been significantly improved. The results indicate that the performances of HOG and HOF, respectively 94.53% and 92.42%, also outperform the state-of-the-art methods, as mentioned in table 3. In addition, lower-cost descriptors like HOG, HOF have more benefits for decreasing computational cost in processes, such as feature extraction and video representation (using the BoW model). These advantages
300 provide a promising way for building effective and efficient systems.
305

6.2. Evaluate the Role of Intensity Representations

In this section, we consider the role of representations to our proposed method. Figure 3 confirms that front representation achieves the best result. Obviously, it is an indispensable component to merge information. For the rest,
310 we perform experiments on representation combinations with front representation. Experimental results are reported in figure 5. In this experiment, the

recognition accuracies of combinations are calculated on each intensity representations and the fusion.

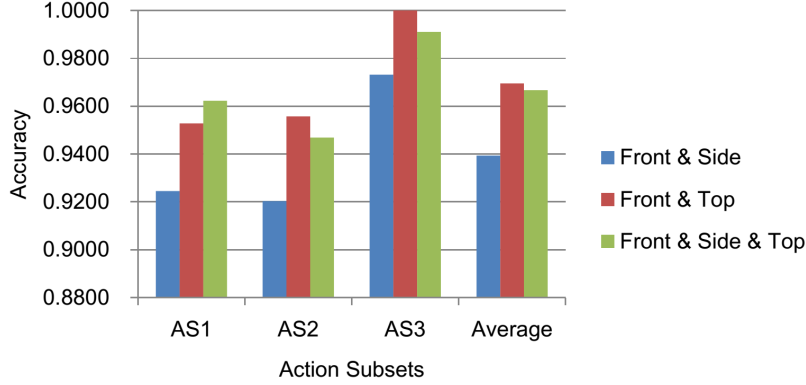


Figure 5: Comparison of recognition accuracy on combinations of intensity representations.

In order to conduct the experiments, we create combinations: front and side,
 315 front and top. Figure 5 indicates that the combination of front and top is better
 than the combination of front and side. More interestingly, the achieved perfor-
 mance, which is 96.95% accuracy, from the combination of front and top beats
 the performance based on combining all the representations, in terms of average.
 Actually, the discovery provides a good choice to decrease computational cost
 320 but still ensures a convincing performance.

6.3. MSR Daily Activity 3D Dataset

The MSR Daily Activity 3D dataset is proposed by [4], which includes 16
 daily activities (Fig. 6) such as talking on the phone, reading a book, playing
 game, ... etc. In this dataset, background objects and subjects appear at
 325 different distances to the camera. Table 6 shows a comparison of recognition
 accuracies between the state-of-the-art methods on MSR Daily Activity 3D
 dataset. In this experiment, we conduct our trajectory-based approach only on
 front representation and use MBH descriptor to describe motion feature. In

addition, we follow the experimental settings as described in [4]. In condition of
 330 only using depth data, [4, 9, 10] report a unexpected performance. In [9], they
 modified this dataset to do evaluation. It is not fair to compare. Therefore, to
 ensure a fair comparison, we follow a framework similar to [9] and evaluate on
 original MSR Daily Activity 3D dataset.

Method	Accuracy
LOP [4]	42.5
HON4D [10]	52
DSTIP&DCSF [9]	56.88
Ours	62.5

Table 6: Comparison of recognition accuracy on MSR Daily Activity 3D Dataset. Notice that
 results are reported in terms of only using depth data.

Although our method outperforms all the state-of-the-art methods, it is not
 335 our aim. It is important to note that why in condition of only using depth data,
 most of methods are failed. When considering failed samples, such as *playing*
a game, *writing on a paper*, and *using a laptop*, we found that most of them
 are confused with action *still*. For *playing a game*, main action focus on motion
 of fingers, it is very difficult to discriminate from depth noise. For *writing on*
 340 *a paper* and *using a laptop*, hand gestures are major actions to present motion
 information. But it is not fortunately, most of the movements are hidden by
 interactive objects (i.e. book, laptop). That is one reason to explain for the
 failure. The second one is performing similar movements with different objects,
 such as *talking on the phone* and *drinking water*. In these cases, objects are
 345 small and textureless, so, it is very difficult to identify them. Therefore, if
 only depending on depth data, it is very challenging to recognize these actions
 exactly. Due to these reasons, in order to improve the performance of recognition
 systems in terms of interaction, adding more information related to interactive
 objects must be necessary.



(a) Reading book



(b) Drinking water



(c) Talking on a phone



(d) Playing game



(e) Writing on a paper



(f) Using a laptop

Figure 6: Some sample actions on MSR Daily Activity 3D dataset.

350 6.4. Early versus Late Fusion in Our Approach

In terms of the fusion, [33] provided an interesting work. In this work, authors evaluated semantic concepts on two fusion schemes: early fusion and late fusion. They conducted experiments on the 2004 TRECVID benchmark dataset for visual modality and textual modality. Results indicated that the performance of the late fusion scheme is better than the performance of the early fusion scheme for most concepts. This evaluation are also applied for several multimodal-based analysis systems. However, the conclusion is reasonable or not for our approach, when considering each intensity representation as a modality. In order to answer this issue, we perform similar experiments on the late fusion scheme. In the experimental settings, we use the MBH descriptor to represent motion features and work on representation combinations: (front and side), (front and top) and (front, side and top). Experimental results in comparison between the early fusion scheme and the late fusion scheme are showed in figure 7.

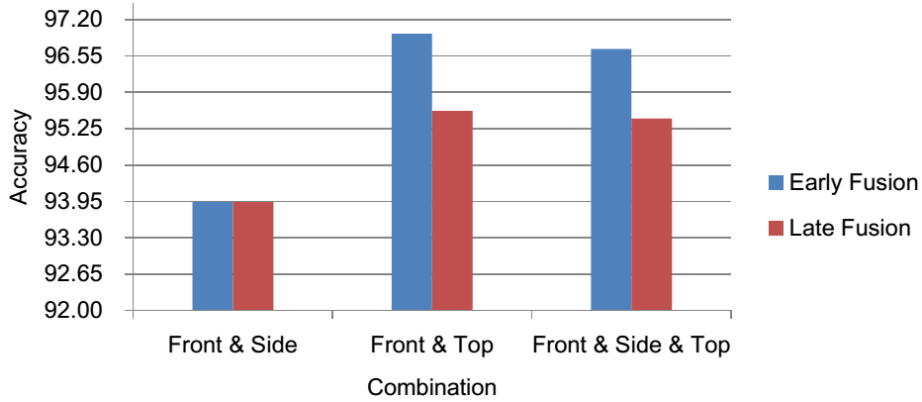


Figure 7: Comparison of recognition accuracy on the early and late fusion schemes.

365 Figure 7 indicates that both of the fusion schemes obtain significant improvements. However, the early fusion scheme gets better performances. Actually, we know that disadvantage of the early fusion approach is the difficulty to create

a good feature representation, due to the semantic difference of modalities. To deal with this challenge, the late fusion approach is used to convert the representations into the same type of semantics (i.e. probability score). In our approach, due to the similarity of semantics between modalities (i.e. features to represent motion information), the performance of the early fusion approach will tend to be better than the one of the late fusion approach. Besides, the achieved results from combinations confirm again that selecting representations to merge motion information is not a trivial task.

7. Conclusions

We proposed the Pseudo-3D Trajectories, a 2D trajectory-based approach, for human action recognition using depth data in this work. We evaluated our approach by using the dense trajectory motion feature on the challenging datasets. More interestingly, our proposed trajectory-based approach only applied for one representation beats all the recent state-of-the-art approaches in terms of depth data. Besides, in order to deal with confused actions due to similar movements, compensating information from other representations is proposed. Therefore, the effectiveness of our approach on depth datasets like MSR is confirmed.

A trajectory-based approach with compensating information from separate representations shows promising results. This opens a general approach to leverage intensity-based techniques for depth data. This also suggests the importance of trajectory-based motion information on human action recognition using depth data. Therefore, exploiting depth-based motion trajectories can be beneficial for action recognition systems using depth cameras. This is also an interesting idea for our future work.

References

- [1] H. Pirsiavash, D. Ramanan, Detecting activities of daily living in first-person camera views, in: Computer Vision and Pattern Recognition (CVPR), 2012 IEEE Conference on, IEEE, 2012, pp. 2847–2854.
- [2] R. Poppe, A survey on vision-based human action recognition, Image and vision computing 28 (6) (2010) 976–990.
- [3] W. Li, Z. Zhang, Z. Liu, Action recognition based on a bag of 3d points, in: Computer Vision and Pattern Recognition Workshops (CVPRW), 2010 IEEE Computer Society Conference on, IEEE, 2010, pp. 9–14.
- [4] J. Wang, Z. Liu, Y. Wu, J. Yuan, Mining actionlet ensemble for action recognition with depth cameras, in: Computer Vision and Pattern Recognition (CVPR), 2012 IEEE Conference on, IEEE, 2012, pp. 1290–1297.
- [5] X. Yang, Y. Tian, Eigenjoints-based action recognition using naive-bayes-nearest-neighbor, in: Computer Vision and Pattern Recognition Workshops (CVPRW), 2012 IEEE Computer Society Conference on, IEEE, 2012, pp. 14–19.
- [6] X. Yang, C. Zhang, Y. Tian, Recognizing actions using depth motion maps-based histograms of oriented gradients, in: Proceedings of the 20th ACM international conference on Multimedia, ACM, 2012, pp. 1057–1060.
- [7] L. Xia, C.-C. Chen, J. Aggarwal, Human detection using depth information by kinect, in: Computer Vision and Pattern Recognition Workshops (CVPRW), 2011 IEEE Computer Society Conference on, IEEE, 2011, pp. 15–22.
- [8] L. Xia, C.-C. Chen, J. Aggarwal, View invariant human action recognition using histograms of 3d joints, in: Computer Vision and Pattern Recognition Workshops (CVPRW), 2012 IEEE Computer Society Conference on, IEEE, 2012, pp. 20–27.

- 420 [9] L. Xia, J. Aggarwal, Spatio-temporal depth cuboid similarity feature for activity recognition using depth camera, in: Computer Vision and Pattern Recognition (CVPR), 2013 IEEE Conference on, IEEE, 2013, pp. 2834–2841.
- [10] O. Oreifej, Z. Liu, Hon4d: Histogram of oriented 4d normals for activity recognition from depth sequences, in: Computer Vision and Pattern Recognition (CVPR), 2013 IEEE Conference on, IEEE, 2013, pp. 716–723.
425
- [11] A. W. Vieira, E. R. Nascimento, G. L. Oliveira, Z. Liu, M. F. Campos, Stop: Space-time occupancy patterns for 3d action recognition from depth map sequences, in: Progress in Pattern Recognition, Image Analysis, Computer Vision, and Applications, Springer, 2012, pp. 252–259.
430
- [12] J. Wang, Z. Liu, J. Chorowski, Z. Chen, Y. Wu, Robust 3d action recognition with random occupancy patterns, in: Computer Vision–ECCV 2012, Springer, 2012, pp. 872–885.
- [13] I. Laptev, On space-time interest points, International Journal of Computer Vision 64 (2-3) (2005) 107–123.
435
- [14] P. Dollár, V. Rabaud, G. Cottrell, S. Belongie, Behavior recognition via sparse spatio-temporal features, in: Visual Surveillance and Performance Evaluation of Tracking and Surveillance, 2005. 2nd Joint IEEE International Workshop on, IEEE, 2005, pp. 65–72.
- 440 [15] I. Laptev, M. Marszalek, C. Schmid, B. Rozenfeld, Learning realistic human actions from movies, in: Computer Vision and Pattern Recognition, 2008. CVPR 2008. IEEE Conference on, IEEE, 2008, pp. 1–8.
- [16] M. Bregonzio, S. Gong, T. Xiang, Recognising action as clouds of space-time interest points, in: Computer Vision and Pattern Recognition, 2009. CVPR 2009. IEEE Conference on, IEEE, 2009, pp. 1948–1955.
445

- [17] A. Klser, M. Marszaek, C. Schmid, A spatio-temporal descriptor based on 3d-gradients, in: Proceedings of the British Machine Vision Conference (BMVC08), Leeds, United Kingdom, September 2008, 2008, pp. 995–1004.
- [18] G. Willems, T. Tuytelaars, L. Van Gool, An efficient dense and scale-invariant spatio-temporal interest point detector, in: Computer Vision–ECCV 2008, Springer, 2008, pp. 650–663.
- [19] P. Matikainen, M. Hebert, R. Sukthankar, Trajectons: Action recognition through the motion analysis of tracked features, in: Computer Vision Workshops (ICCV Workshops), 2009 IEEE 12th International Conference on, IEEE, 2009, pp. 514–521.
- [20] R. Messing, C. Pal, H. Kautz, Activity recognition using the velocity histories of tracked keypoints, in: Computer Vision, 2009 IEEE 12th International Conference on, IEEE, 2009, pp. 104–111.
- [21] J. Sun, X. Wu, S. Yan, L.-F. Cheong, T.-S. Chua, J. Li, Hierarchical spatio-temporal context modeling for action recognition, in: Computer Vision and Pattern Recognition, 2009. CVPR 2009. IEEE Conference on, IEEE, 2009, pp. 2004–2011.
- [22] N. Dalal, B. Triggs, Histograms of oriented gradients for human detection, in: Computer Vision and Pattern Recognition, 2005. CVPR 2005. IEEE Computer Society Conference on, Vol. 1, IEEE, 2005, pp. 886–893.
- [23] J. Shotton, T. Sharp, A. Kipman, A. Fitzgibbon, M. Finocchio, A. Blake, M. Cook, R. Moore, Real-time human pose recognition in parts from single depth images, Communications of the ACM 56 (1) (2013) 116–124.
- [24] H. Wang, A. Kläser, C. Schmid, C.-L. Liu, Action Recognition by Dense Trajectories, in: IEEE Conference on Computer Vision & Pattern Recognition, Colorado Springs, United States, 2011, pp. 3169–3176.
URL <http://hal.inria.fr/inria-00583818/en>

- [25] B. D. Lucas, T. Kanade, et al., An iterative image registration technique with an application to stereo vision., in: IJCAI, Vol. 81, 1981, pp. 674–679.
- 475 [26] S. Phan, T. D. Ngo, V. Lam, S. Tran, D.-D. Le, D. A. Duong, S. Satoh, Multimedia event detection using segment-based approach for motion feature, Journal of Signal Processing Systems 74 (1) (2014) 19–31.
- [27] D. Oneata, M. Douze, J. Revaud, S. Jochen, D. Potapov, H. Wang, Z. Harchaoui, J. Verbeek, C. Schmid, R. Aly, et al., Axes at trecvid 2012: Kis, 480 ins, and med, in: TRECVID workshop, 2012.
- [28] P. Natarajan, P. Natarajan, S. Wu, X. Zhuang, A. Vazquez-reina, S. N. Vitaladevuni, C. Andersen, R. Prasad, G. Ye, D. Liu, et al., Bbn viser trecvid 2012 multimedia event detection and multimedia event recounting systems.
- 485 [29] G. Farnebäck, Two-frame motion estimation based on polynomial expansion, in: Image Analysis, Springer, 2003, pp. 363–370.
- [30] N. Dalal, B. Triggs, C. Schmid, Human detection using oriented histograms of flow and appearance, in: Computer Vision–ECCV 2006, Springer, 2006, pp. 428–441.
- 490 [31] H. Wang, M. M. Ullah, A. Klaser, I. Laptev, C. Schmid, et al., Evaluation of local spatio-temporal features for action recognition, in: BMVC 2009-British Machine Vision Conference, 2009.
- [32] J. Liu, J. Luo, M. Shah, Recognizing realistic actions from videos in the wild, in: Computer Vision and Pattern Recognition, 2009. CVPR 2009. 495 IEEE Conference on, IEEE, 2009, pp. 1996–2003.
- [33] C. G. Snoek, M. Worring, A. W. Smeulders, Early versus late fusion in semantic video analysis, in: Proceedings of the 13th annual ACM international conference on Multimedia, ACM, 2005, pp. 399–402.